16

Liquid- and Gas-Phase Separation in MOFs

16.1 Introduction

Many industrial processes such as the purification of feedstock for the chemical industry, fuels, energy carriers, and exhaust gases as well as purification processes finding application in our daily life such as the purification of drinking water are based on separation. Most of these processes use porous solids for the selective separation of specific components from influent gaseous or liquid mixtures to give high-purity products.

Gases such as hydrogen, methane, and light hydrocarbons are sources of energy and are used in combustion engines or fuel cells [1]. This is, however, only possible if they are supplied in high purity. In Chapter 13 we discussed the problem of increasing CO_2 levels in the atmosphere and the application of metal-organic frameworks (MOFs) in CO_2 capture. This process is thermodynamically controlled (i.e. equilibrium adsorption), just like the purification of natural gas, syngas, and the separation of light hydrocarbons. In contrast, the separation of gaseous mixtures of different isomers of hydrocarbons is typically controlled by kinetics (Figure 16.1). A further development in terms of separation processes based on porous solids are mixed-matrix membranes (MMMs): composite membranes made from a polymer (membrane) and porous solid additives (filler). MMMs combine both the selectivity of porous adsorbents such as MOFs, zeolitic imidazolate frameworks (ZIFs), and covalent organic framework (COF) with the flux, facile preparation, and flexibility of polymers. They have been tested for many separation processes and their high performance illustrates how hybrid materials can surpass the performance of their individual components and in some cases also their sum [2].

MOF-based separation processes are not only applicable to gaseous mixtures but also to the separation of mixtures of liquids and the selective removal of specific components from them. In this context, the removal of biologically active molecules from aqueous solution is becoming increasingly important. Trace amounts of medical drugs and other biologically active molecules in rivers and drinking water worldwide pose a significant health concern [3]. Another example for a potential application of porous solids in the separation of liquids is the purification of liquid fuels, petroleum, and shale oil. They all contain cyclic amines that negatively influence their quality due to bad odor, acute

Introduction to Reticular Chemistry: Metal-Organic Frameworks and Covalent Organic Frameworks,
First Edition. Omar M. Yaghi, Markus J. Kalmutzki, and Christian S. Diercks.

Companion website: www.wiley.com/go/yaghi/reticular

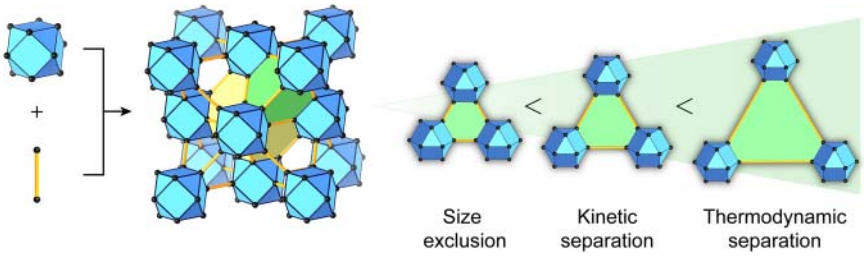

Figure 16.1 The predominant mechanism for separation is correlated to the ratio of the pore size and the kinetic diameter of the components in the mixture. While all three mechanisms can afford the separation of gas/liquid mixtures, only thermodynamic separation allows to selectively capture a specific component within the pores.

aquatic toxicity and carcinogenicity, and the increase formation of deposits. The combustion of fuels containing cyclic amines, or amines in general, leads to the formation of nitrous oxides (NO_x), which are the cause of acid rain [4].

To show high performance in the abovementioned processes, materials with high selectivity in the respective application must be developed. The rapidly growing number of compounds made by means of reticular chemistry show great promise for gas and liquid phase separation. Their facile synthesis in combination with unique structural and physical features compared to traditional porous materials (e.g. zeolites and porous carbons) makes them ideal for gas separation and the selective capture of molecules from the gas or liquid phase. These features include rational design approaches (see Chapters 4 and 5), the possibility to deliberately introduce functional sites (see Chapter 6), and ultra-high porosities with BET surface areas of over 6000 $m^2\ g^{-1}$ (see Chapter 2). The basic physical processes involved in the separation of gases and liquids in porous solids have been discussed in Chapter 13. Here, we will take a closer look at the separation of volatile organic molecules such as light hydrocarbons, aromatic compounds, and the adsorptive removal of bioactive molecules from water.

16.2 Separation of Hydrocarbons

Hydrocarbons are used as feedstock for the chemical industry and the separation of mixtures of hydrocarbon is one of the most important processes in the petrochemical industry [5]. Hydrocarbons are exclusively composed of carbon and hydrogen, and are categorized into alkanes (paraffins), alkenes (olefins), and aromatic hydrocarbons (naphthenic hydrocarbons). Many olefins (e.g. ethylene, propylene, and butadiene) and naphthenic hydrocarbons (e.g. benzene, toluene, and xylene) are important feedstocks for the chemical industry. *p*-Xylene is used as the starting material for the industrial synthesis of terephthalic acid (H_2BDC), which is an important component of many polymers such as PET (polyethyleneterephthalate) and also finds use in MOF chemistry as a linker [6]. The widespread industrial use of light hydrocarbons (C_1–C_4 fraction), isomers of alkanes, and especially C_8 naphthenic hydrocarbons (ethylbenzene, *o*-xylene,

m-xylene, and *p*-xylene) highlights the importance of selective separation processes for the isolation of these compounds in pure phase.

The separation of alkane/alkene mixtures is commonly realized by cryogenic distillation. This process not only requires a large number of distillation stages and a high reflux ratio to obtain fractions of high purity but also operates at high pressures and cryogenic temperatures. These factors render cryogenic distillation less economical. In a similar manner, the separation of C_8 naphthenic hydrocarbons by distillation from an extracting solvent under reduced pressure is cost intensive, which renders the synthesis of these compounds (e.g. synthesis of ethylbenzene from ethylene and benzene) more profitable. This is also rooted in the fact that the separation of C_6 from C_7 and C_8 hydrocarbons is comparatively simple.

Natural gas contains different hydrocarbons such as methane (87–97%), ethane (1.5–9%), propane (1–1.5%), *iso*-butane (0.01–0.3%), and *n*-butane (0.01–0.3%) and the separation of methane from the other components is an essential industrial process. This is because all hydrocarbons present in natural gas have higher value as pure phase compounds that can be used as feedstock for the chemical industry (e.g. ethane, propane, *iso*-butane, etc.) or higher quality fuels (e.g. methane). C_2 and C_3 hydrocarbons are important raw materials for various products, such as acetic acid and polymers including rubbers and plastics. High-purity natural gas allows for a cleaner, more efficient combustion and consequently lower CO_2 emissions.

Separation using porous solids provides a more (cost) efficient alternative to the expensive processes outlined above. One key factor here is the structural tunability of MOFs, which enables the precise adjustment of a variety of parameters such as the shape, metrics, polarity, and functionality of the pores. Such control is not present in the inorganic and carbon-based materials that are currently employed in industrial separation processes. Aside from the tunability, MOFs can exhibit sensitivity toward external stimuli such as pressure or temperature that result in a gate-opening or breathing motion of the whole framework. This degree of flexibility can lead to an outstanding selectivity and performance in separation processes that is not possible with rigid porous materials (i.e. zeolites and porous carbon). In the following, we will develop principles for the design of potent MOFs and ZIFs with respect to the separation of light hydrocarbons (Section 16.2.1), light olefins and paraffins (Section 16.2.2), and aromatic C_8 hydrocarbons (Section 16.2.3).

16.2.1 C_1–C_5 Separation

The separation of C_1–C_5 hydrocarbons can be achieved in different ways. Here, we will focus on the adsorptive separation based on van der Waals interactions between the gas molecules and the pore surface. According to theoretical studies the enthalpy and entropy of adsorption become more negative with increasing chain length of the hydrocarbon [7]. Therefore, long alkane chains are adsorbed more strongly until the selectivity reaches a maximum at a certain pressure P/P_0 (Figure 16.2). When the pressure is further increased, the entropic cost of ordering the long alkane chains outweighs the enthalpic advantage. Similar results are

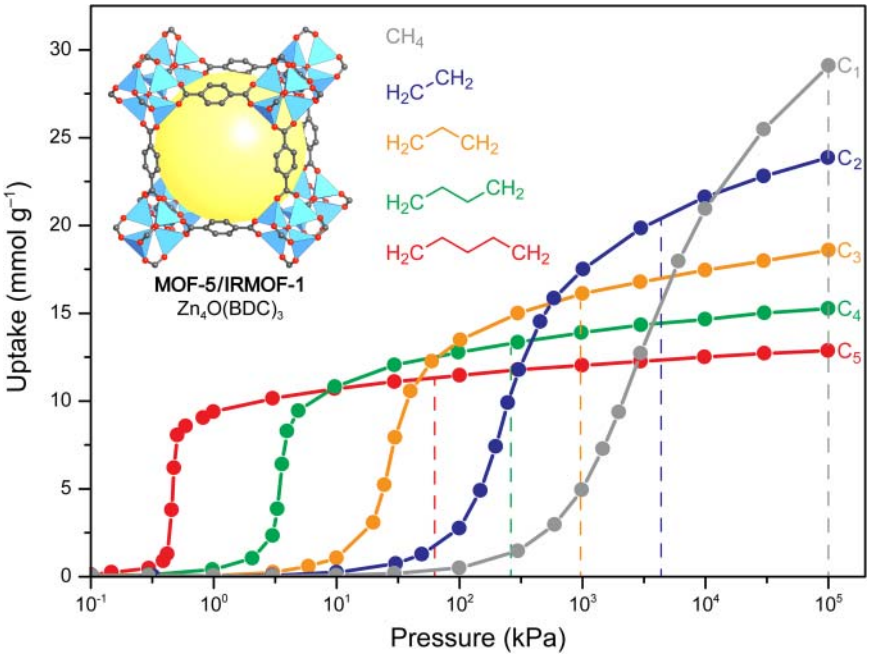

Figure 16.2 Calculated adsorption isotherms of linear C_1–C_5 alkanes in MOF-5 at 300 K [7]. In the low pressure region the high enthalpy of adsorption for long alkane chains outweighs the entropic cost of ordering them. At higher pressures the uptake of lower alkanes increases. The dotted lines represent the bulk saturation pressure of the corresponding component. Color code for isotherms: C_1, red; C_2, green; C_3, orange; C_4, blue; C_5, gray. The crystal structure of MOF-5 is shown in the insert. Color code: Zn, blue; C, gray; O, red.

observed in experimental studies for the adsorption of *n*-butane and methane in MOF-5 and HKUST-1 [8]. In both cases, the isosteric heat of adsorption is more than two times higher for *n*-butane ($Q_{st} = -23.6$ and $-29.6\,kJ\,mol^{-1}$) than for methane ($Q_{st} = -10.6$ and $-12.0\,kJ\,mol^{-1}$) [9].

Simulations reveal a dependence of the adsorption behavior on different structural factors [10]. The adsorption capacity in isoreticular MOFs is mainly correlated to the pore size, and a consequential decrease in the selectivity with increasing length of the linker is observed. For MOFs built from linkers of the same length, the strength of the interaction is correlated to the number of carbon atoms in the linker, which results in an increase in the selectivity for linkers with a larger aromatic backbone. This is illustrated by the example in Figure 16.3 showing the selectivity for methane in MOF-5 and the hypothetical isoreticular IRMOF-993 ($Zn_4O(ADC)_3$, where ADC = 9,10-anthracene dicarboxylate) [10, 11]. These results however cannot be confirmed experimentally because the reticulation of H_2ADC and Zn^{2+} yields PCN-13 rather than IRMOF-993. PCN-13 has a limited pore size of only 3.5 Å and therefore different gas adsorption properties (Figure 16.3a) [12].

Flexible MOFs commonly show steps in their adsorption isotherms due to swelling, gate-opening, or breathing effects. The MIL-53 family is a prominent

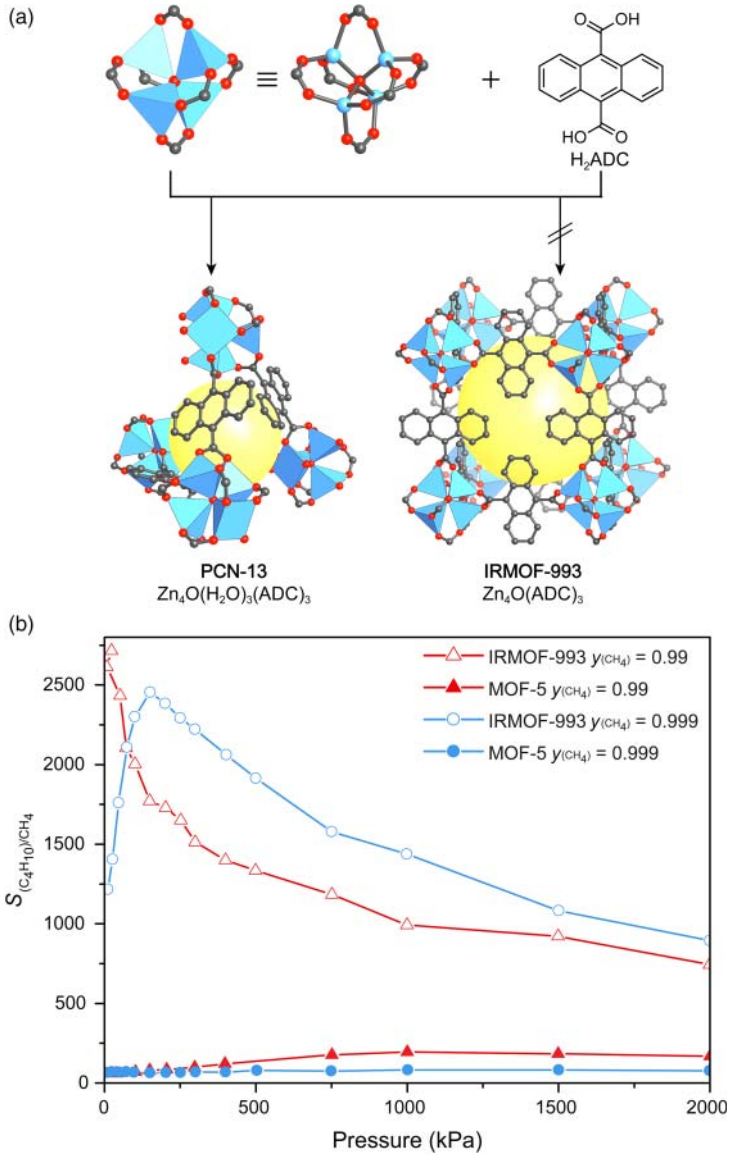

Figure 16.3 (a) Comparison of the crystal structures of PCN-13 and that of the hypothetical IRMOF-993. Only one pore is shown and all hydrogen atoms are omitted for clarity. IRMOF-993 cannot be prepared but serves as a good model for theoretical considerations regarding the correlation between the size of the aromatic backbone of the linker and the selectivity with respect to linear alkanes. (b) Comparison of the selectivity of MOF-5 (filled symbols) and IRMOF-933 (open symbols) in the removal of trace amounts of *n*-butane from methane as a function of the bulk pressure (triangles $y_{(CH_4)} = 0.99$; circles $y_{(CH_4)} = 0.999$).

example for this type of adsorption behavior. For the adsorption of *n*-propane through *n*-nonane the adsorption isotherms of MIL-53(Cr) (at 303 K) show an additional steep step at different pressures depending on the gas used, which is not observed for smaller hydrocarbons (methane and ethane) and is thus attributed to framework swelling [13]. MAMS-1 (Ni_8(5-BBDC)$_6$(μ_3-OH)$_4$, where BBDC = 5-tert-butyl-1,3-benzenedicarboxylate), the first MOF-based mesh-adjustable molecular sieve, can discriminate methane/ethane and ethane/propane mixtures with high selectivity. Here, the selectivity is rooted in the capability of this framework to undergo a phase transition from a narrow pore (*np*) to a wide pore (*wp*) phase, also known as gate-opening [14]. The structure of MAMS-1 consists of hydrophobic gas storage chambers that are connected through hydrophilic channels. Influent gas molecules can enter the hydrophobic gas storage chambers only through their interface with the hydrophilic channels. Consequently, most gas is stored within these chambers. Each channel–chamber interface is framed by four BBDC linkers that act as a gate (Figure 16.4a,b). The thermally induced gate-opening effect in MAMS-1 is controlled by the amplitude of thermal vibration. The correlation between the width of the gate and the temperature gives rise to an equation that predicts the diameter of the gate for any given temperature. The diameter can vary between 2.9 and 5.0 Å, making it possible to separate methane and ethane from propane and butane, or methane from ethane, propane, and butane, depending on the temperature (Figure 16.4c).

In summary, for the adsorption of alkanes in MOFs, S-shaped Type-IV (and V) adsorption isotherms are often observed. Steep adsorption steps that occur at different pressures for different gases are utilized for their separation. A stronger adsorption is observed for longer alkane chains, and the adsorption capacity is usually higher for shorter alkanes because their smaller size increases the maximum loading. In contrast, the lower molecular surface decreases the strength of van der Waals interactions. These principles are used to facilitate the separation of a wide range of alkane mixtures. For more detailed information on specific separations, the reader is referred elsewhere [15].

16.2.2 Separation of Light Olefins and Paraffins

The separation of olefin/paraffin mixtures represents some of the most energy-intensive processes in the petrochemical industry [16]. Their similar molecular sizes, weights, and volatilities make these processes especially difficult. Alternative adsorption-based processes present the potential to significantly reduce operating expenses due to lower energy consumption. For this purpose, a number of adsorbents, mainly zeolites, have been evaluated, but only a few of them are capable of the kinetic separation of olefin/paraffin mixtures [17]. In contrast to most of the traditional adsorbents, MOFs often display a stronger affinity for saturated over unsaturated hydrocarbons in single component isotherms and their initial capacity is typically restored by regeneration using pressure-, vacuum-, and/or temperature-swing adsorption (PSA, VSA, and TSA). Employing materials that show this type of selectivity in the separation of olefin/paraffin mixtures leads to high-purity paraffins that

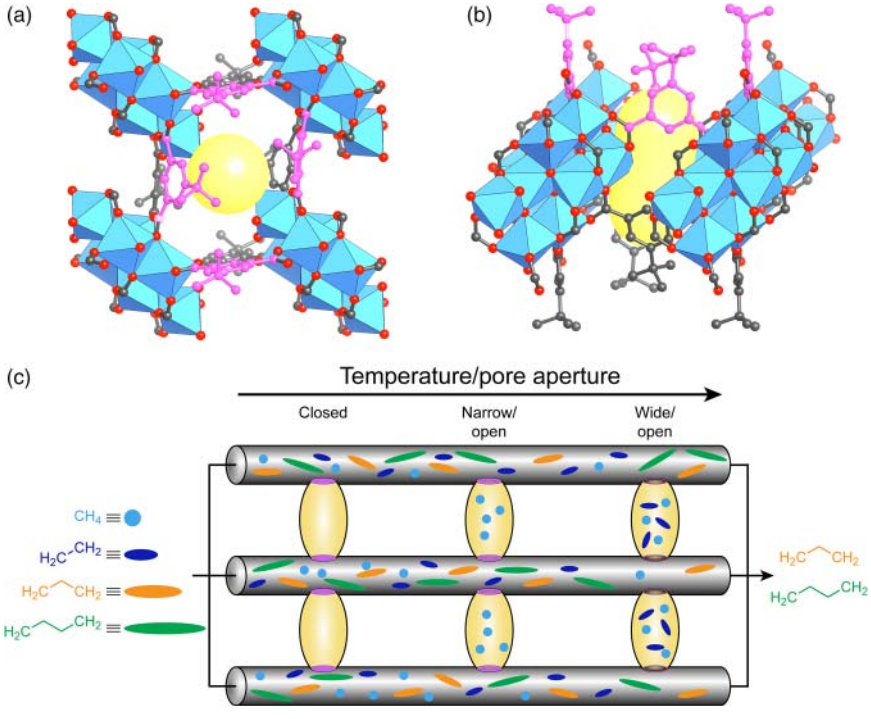

Figure 16.4 (a, b) Top and side view of the intersection connecting the hydrophilic 1D pores and the hydrophobic chambers. The BBDC linkers lining the opening of their intersections are highlighted in pink. (c) Schematic separation of C_1–C_4 alkanes in MAMS-1. The closed pores exclude any of the components from entering the hydrophobic chambers (left). Increasing the temperature results in a larger diameter of the intersection, allowing methane to pass into the hydrophobic chambers (center). A further increase in temperature results in intersection apertures large enough to allow for methane and ethane to enter the hydrophobic chambers (right). Propane and ethane are too large to enter the hydrophobic storage chambers and are excluded.

are required for polymerization processes. Such separation processes can be performed following four different mechanisms: (i) adsorptive or thermodynamic equilibrium separation, (ii) kinetic separation, (iii) separation based on gate-opening effects, and (iv) separation by molecular sieving. In the following, we will discuss these four mechanisms separately and highlight their material requirements.

16.2.2.1 Thermodynamic Separation of Olefin/Paraffin Mixtures

Thermodynamic separation relies on the selective adsorption of one component of the mixture over another. Open metal sites also play an important role in the separation of olefin/paraffin mixtures following a thermodynamic mechanism. This is because light olefins and paraffins such as ethane and ethylene are typically equally polarizable, possess no or only a small dipole moment, and generally have small quadrupole moments, and therefore strong adsorption sites (e.g. open metal sites) are required to increase the selectivity. This is however not always

true, as illustrated by the fact that the preferential adsorption of ethylene over ethane in HKUST-1 is mainly correlated to stronger hydrogen bonding between ethylene and the basic oxygen atoms of the secondary building units (SBUs) and only partially to electrostatic interactions with copper open metal sites [18].

The isosteric heats of adsorption for ethane and ethylene differ only by approximately 3 kJ mol^{-1}, which leads to a low selectivity factor of 2 [19]. In a similar manner, the separation of propane and propylene reveals a preferential binding of propylene but with a larger difference in the isosteric heats of adsorption of about −13 kJ mol^{-1} [20]. Here, the stronger adsorption of propylene is attributed to the presence of open metal sites that give rise to an interaction between the bonding p-orbitals in propylene and the vacant copper s-orbitals [20, 21]. Evaluation of the potential of HKUST-1 for the separation of various olefin/paraffin mixtures (ethane/ethylene, propane/propylene, and *iso*-butane/*iso*-butylene) by simulated moving bed, PSA, and VSA reveals preferential adsorption of the unsaturated component [15b, 16, 21b, 22]. Similar behavior is observed for other MOFs with open metal sites. In the separation of olefin/paraffin mixtures using fully activated (Fe)MIL-100, adsorption of the olefin is typically favored [23].

From a practical point of view, alkane-selective adsorbents are favorable because it is hard to recover the desired alkene product from olefin-selective sorbents, and multiple separation cycles must be performed to obtain high-purity products such as those required to produce polymer grade polyethylene and polypropylene. The same separations can be realized within one cycle using alkane-selective adsorbents. There are, however, only very few MOFs that favor the adsorption of paraffins over olefins. One such MOF is MAF-49 [24]. The selectivity of MAF-49 for ethane over ethylene has its origin in the presence of multiple electronegative and electropositive groups that cover the inner pore surface. Ethane can form six C–H···N hydrogen bonds with these groups whereas ethylene can only form four hydrogen bonds. This means that the favored binding of ethane over ethylene is a result of the spatial arrangement of hydrogen bond acceptors in the pores of MAF-49.

To circumvent the adsorption of unsaturated over saturated species, the separation of olefin/paraffin mixtures in MOFs can also be realized under kinetic control, utilizing the gate-opening effect, or by taking advantage of shape selectivity and size exclusion. Separations following these mechanisms typically show lower selectivity. The highest selectivity is observed for adsorptive separation by MOFs with a high density of open metal sites.

16.2.2.2 Kinetic Separation of Olefin/Paraffin Mixtures

The selective separation of olefin/paraffin mixtures based on a kinetic mechanism makes use of the differences in diffusivities of the individual components of a mixture. Whether a separation process is governed by thermodynamics or kinetics can be assessed by analyzing single-component adsorption isotherms and conducting diffusion studies (see Chapter 13). A separation process is controlled by kinetic effects if the uptake and Q_{st} values for all components of the mixture are similar, but their diffusivities differ significantly.

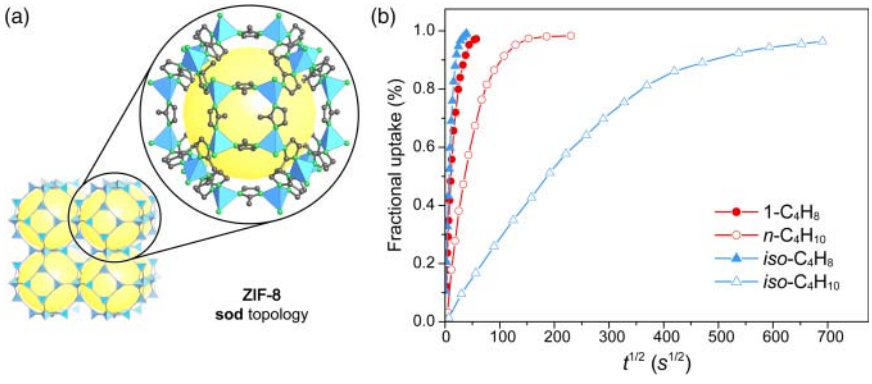

Figure 16.5 (a) Topological representation of the augmented sodalite (**sod**) net and one cage (**tro**) of the structure of ZIF-8. (b) Kinetic uptake curves in ZIF-8 recorded at 35 °C. The red curves represent the kinetic uptake of 1-C_4H_8 (closed symbols) and *n*-C_4H_{10}, and the blue curves represent the kinetic uptake curves of *iso*-C_4H_8 (closed symbols) and *iso*-C_4H_{10} (open symbols), respectively. A higher affinity toward the unsaturated components (1-propylene and *iso*-butylene) compared to the saturated counterparts (*n*-propane and *iso*-butane) is observed.

Kinetic separation is observed for propane/propylene mixtures using three isostructural ZIFs, $Zn(mIM)_2$ (ZIF-8, mIM = 2-methyle imidazolate), $Zn(cIM)_2$ (cIM = 2-chlorolimidazolate), and $Zn(bIM)_2$ (bIM = 2-bromolimidazolate) (Figure 16.5) [25]. Sieving materials such as ZIF-8 show a behavior similar to materials operation on an adsorptive mechanism where generally the unsaturated component is retained due to stronger interactions with its π-system. This finding is correlated to the effective size of the pore opening, giving rise to a significant difference in the diffusion rates for propylene and propane by a factor of 125. Interestingly, C_4 hydrocarbons (*n*-butane, *iso*-butane, *iso*-butene), which are significantly larger than the effective pore aperture for sieving (4.0–4.2 Å), can diffuse into the micropores of ZIF-8. The high kinetic selectivity of ZIF-8 in the separation of *iso*-butene/*iso*-butane and *n*-butane/*iso*-butane mixtures (at 308 K) of up to 180 and 2.5×10^6, respectively, has its origin in the combination of flexibility and dilation of the aperture [26]. Owing to its high performance in the separation of olefin/paraffin mixtures, ZIF-8 is one of the most popular MOFs for the fabrication of MMMs [27].

MOFs with pillared-layered structures are interesting for separation processes because here functionalization can give rise to anistropic diffusion properties. The stacking of 2D layers through pillars (typically N- or O-donor linkers) allows for the adjustment of the interlayer distance, which defines the pore diameter of the channels running parallel to the 2D layers. The pore diameter has a stark influence on the diffusivity of the permeating molecules, and its modification can therefore be utilized to adjust the selectivity in kinetic separation processes. Here we illustrate this concept for the separation of propane/propylene mixtures using a series of isostructural pillared-layered MOFs [28]. The structures of all

MOFs of this particular series are built from **sql** layers of $Zn_2(-COO_2)_4$ paddle wheel SBUs that are connected by BTEB (tetrakis(carboxyphenyl)benzene) linkers, and pillared along the *c*-direction by *R*-BPEE (dipyridylethene derivatives). The layered nature of these materials results in a plate-like crystal morphology (Figure 16.6a,b). The combination of different substitution patterns of both linkers gives rise to a series of MOFs with different pore apertures that can be controlled individually (Figure 16.6b). The modulation of the pore apertures has a significant effect on the kinetic selectivity in the separation of propane/propylene mixtures. The channels in the highly anisotropic structures have different pore

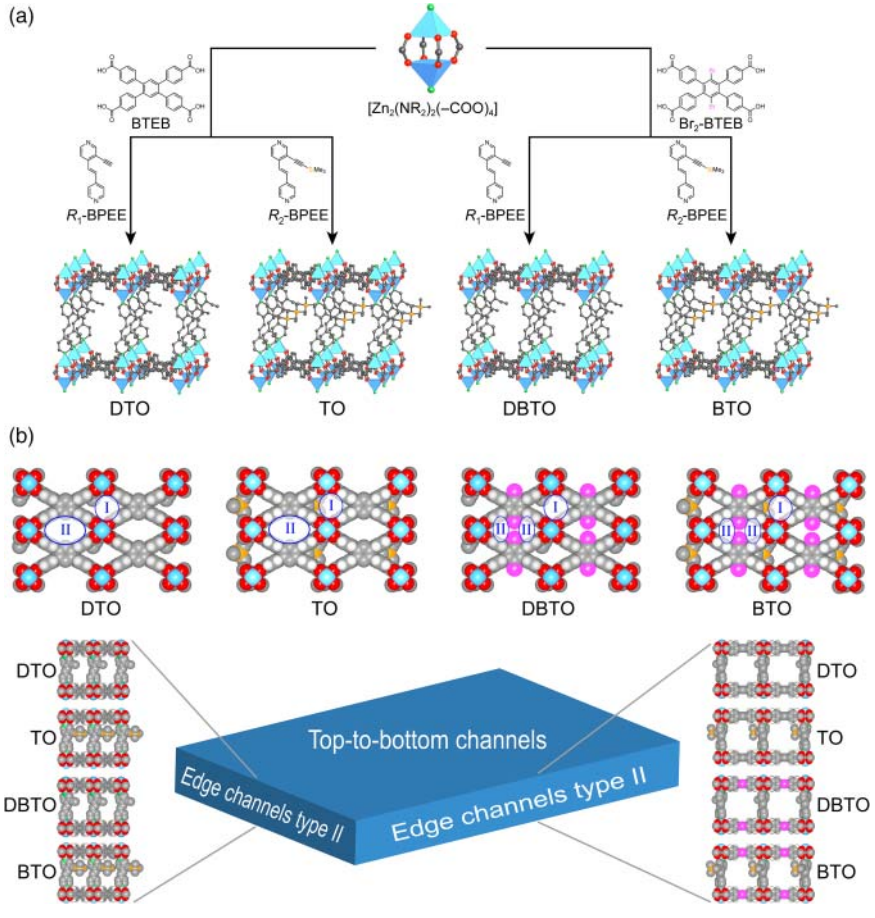

Figure 16.6 (a) Crystal structures of a series of isoreticular functionalized pillared-layered MOFs. The structures are built from **sql** layers of zinc paddle wheel SBUs that are connected by tetratopic BTEB or Br_2-BTEB linkers. These layers are pillared by pyridine-based struts (*R*-BPEE) to form the 3D frameworks DTO, TO, DBTO, and BTO (**fsc** topology). (b) All four compounds form crystals of plate-like morphology. Owing to the morphology of the crystals separation mainly occurs in the small channels (I) and (II), the larger edge-to-edge channels do not contribute to the separation. A top view of all types of channels is given and their orientation in the crystal is indicated.

diameters and run along all three directions of the plate-like crystals. Because the exposed surface of the different faces of the plate-like crystals are not identical, separation occurs mainly in the small channels I and II that run parallel to the BPEE linkers, from the top to the bottom face of the crystal (Figure 16.6b). The aperture of channel II is controlled by the substitution pattern of the BTEB linker while the apertures of channel I and the edge channels are controlled by substituents appended to the BPEE linker. Frameworks that are prepared using Br_2-BTEB display a higher selectivity in the separation of propane/propylene mixtures, which is attributed to the decreased pore aperture of channel II. This is supported by the fact that grinding the material leads to a significantly lower selectivity caused by the reduced "top-to-edges surface" ratio of the crystals.

16.2.2.3 Separation of Olefin/Paraffin Mixtures Utilizing the Gate-Opening Effect

Separation utilizing the gate-opening effect of framework structures also relies on differences in the diffusivity in a way similar to the kinetic separation mechanism outlined above. In contrast to this mechanism, the selectivity for paraffins is attributed to a gate-opening effect that controls the uptake and release of specific molecules at specific gate-opening pressures. In this context, ZIFs are interesting materials that can perform the separation of light hydrocarbons by gate-opening. ZIF-7 ($Zn(BIM)_2$, BIM = benzimidazolate) selectively adsorbs paraffins over olefins. This selectivity arises from interactions between the adsorbate molecules and the benzene rings of the BIM linkers that point into the narrow pore windows [29]. The gate-opening effect triggered by this interaction results in selective discrimination between molecules of similar size but (slightly) different shapes and facilitates the rapid desorption of the adsorbed species at relatively low temperatures. The difference in the adsorption behavior of different adsorbents is mainly correlated to their ability to form "adsorption complexes" at the external surface of the pore openings of ZIF-7 [29a, 30].

RPM3-Zn ($Zn_2(BPDC)_2(BPEE)$), a pillared-layered MOF, is another example for selective separation of ethane/ethylene mixtures based on the gate-opening effect. RPM3-Zn is built from dinulcear $Zn_2(–COO_2)_4$ paddle wheel SBUs that are connected by BPDC linkers to form **sql** layers, which are pillared by BPEE struts to form a framework with an overall **pcu** topology [31]. The adsorption isotherms for olefins and paraffins both show stepwise adsorption and pronounced hysteresis at specific gate-opening pressures and the gate-opening pressure itself strongly depends on the chain length of the adsorbate [32]. Gate-opening in RPM3-Zn is caused by hydrogen bonding between the methylene groups of ethylene and the end-on coordinated carboxylate oxygen of the BPDC linker as evidenced by Raman spectroscopy and density functional theory calculations.

16.2.2.4 Separation of Olefin/Paraffin Mixtures by Molecular Sieving

The presence of pores that are significantly smaller than the kinetic diameter of at least one of the components of the gas mixture can be used for its separation by molecular sieving. While ZIF-7 and ZIF-8 only show high selectivity up

to a characteristic gate-opening pressure, materials with pore apertures that allow for the selective exclusion of molecules above a specific size limit (i.e. size exclusion) must be designed to facilitate this kind of selectivity over a larger pressure range. One such material is KAUST-7 ($Ni(Pyr)_2(NbOF_5)$, also referred to as NbOFFIVE-1-Ni, where Pyr = pyrazine)) [33].[1] KAUST-7 has a pillared-layered structure built from **sql** layers of 6-coordinated nickel centers that are connected through Pyr linkers. These layers are pillared by inorganic $NbOF_5$-units to form a 3D framework of **pcu** topology and shows structural similarity to SIFSIX-3-Ni ($Ni(Pyr)_2(SiF_6)$) (Figure 16.7). The bulkier $NbOF_5$ units in the structure of KAUST-7 result in smaller pore apertures (3.047 Å) compared to that of SIFSIX-3-Ni (5.032 Å). The restricted pore size facilitates the exclusion of propane molecules whereas the slightly smaller propylene molecules can diffuse through the material. Consequently, KAUST-7 displays complete molecular exclusion of propane from a propane/propylene mixture at ambient temperature and atmospheric pressure.

16.2.3 Separation of Aromatic C_8 Isomers

Aromatic C_8 hydrocarbons such as xylene isomers and ethylbenzene are important feedstock chemicals for the synthesis of polymers and other value-added chemicals. Therefore, their selective and efficient separation is of great interest for the petrochemical industry. Figure 16.8 shows aromatic C_8 hydrocarbons and industrial products synthesized from them. Phthalic anhydride, a plasticizer in polymers, is synthesized from *o*-xylene. The oxidation of *m*-xylene yields isophthalic acid, more recently used in the synthesis of PET resin blends. *p*-Xylene (PX) is used to produce terephthalic acid, a basic component for the production of PET. Ethylbenzene is dehydrogenated to styrene and subsequently polymerized to give polystyrene.

The separation of aromatic C_8 hydrocarbons by distillation is energy intensive and requires enormous columns with about 150–200 plates and a high reflux ratio [34]. Research on adsorptive separation of aromatic C_8 hydrocarbons using zeolites indicates that this process may provide a more economical alternative. Consequently, MOFs and ZIFs have been intensely studied with respect to this application.

In the separation of a mixture of aromatic C_8 hydrocarbons ZIF-8 shows a selectivity of 4.0 and 2.4 for mixtures of *p*-/*o*-xylene and *p*-/*m*-xylene, respectively (see Figure 16.5) [35]. Considering that the pore aperture of ZIF-8 is approximately 3.4 Å in diameter, none of the aromatic C_8 hydrocarbons should be able to diffuse into the pores. However, the imidazolate linkers lining the 6-membered rings in the sodalite (**sod**) structure of ZIF-8 can act like saloon doors, resulting in an increase in the effective pore aperture to about 6.4 Å. This value is close to the kinetic diameter of *p*-xylene and thus enables the separation of xylene isomers owing to a significant difference in their diffusivities [36].

---

1 Strictly speaking, KAUST-7 is a coordination network, since its structure is built from single metal nodes that are connected through neutral pyrazine linkers to form **sql** layers. The pillar is an inorganic unit.

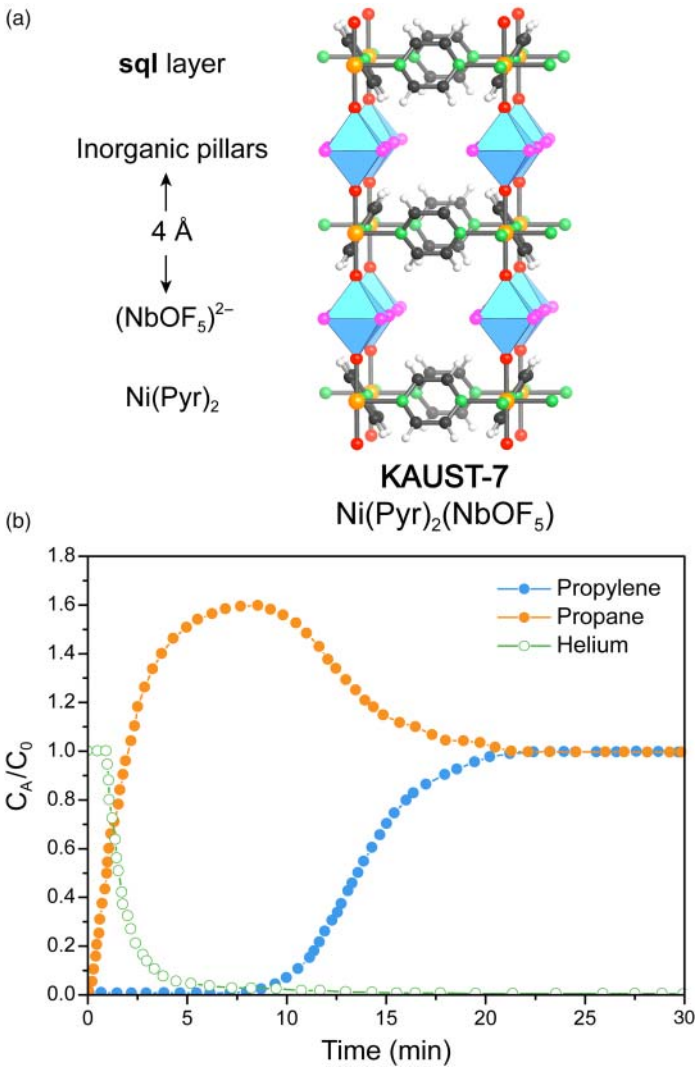

Figure 16.7 (a) Crystal structure of KAUST-7 highlighting the pillared-layered structure. The pyrazine linkers are tilted due to the use of the large $(NbOF_5)^{2-}$ leading to a short distance between neighboring two $(NbOF_5)^{2-}$ building units that belong to adjacent layers. (b) Breakthrough curve for the separation of a propane/propylene mixture illustrating the high selectivity of KAUST-7 for propylene over propane. Color code: Nb, blue; Ni, orange; F/O, red; O, pink; C, gray; N, green.

Compared to ZIFs, MOFs offer a higher degree of structural and functional tunability owing to the almost infinite number of possible SBU–linker combinations. This structural diversity offers great potential for the discovery of materials with high selectivity in the separation of aromatic C_8 hydrocarbons. To design para-selective MOFs, (computational) screening of MOF structures constructed from cages that have apertures in the size regime of the kinetic diameter of xylene

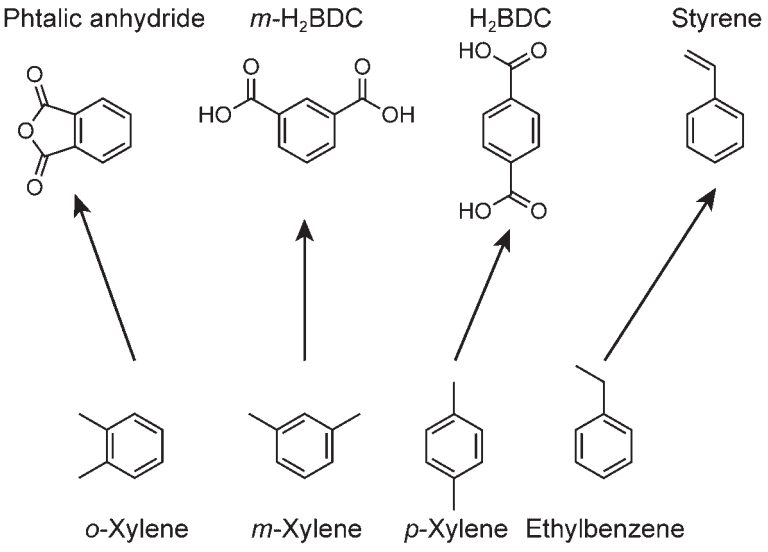

Figure 16.8 Aromatic C_8 hydrocarbons (bottom) alongside industrial products prepared therefrom (top). All compounds shown in the top row are important constitutents of polymers and thus produced in large quantities.

isomers is instructive. In the following, we will elaborate on selected MOFs that fulfill this requirement.

The 1D channels in JUC-77, (In(OH)(OBA) where H_2OBA = 4,4′-oxybis (benzoic acid)) have openings of 10.8 × 7.3 Å, which is close to the kinetic diameters of the xylene isomers. In the separation of xylene isomers, these channels act as molecular sieves that only allow the diffusion of *p*-xylene (the isomer with the smallest width) whereas *m*-xylene and *o*-xylene are excluded due to their larger size [37]. (Ti)MIL-125 and some of its derivatives also show potential for C_8 separation [38]. Here, the high para-selectivity originates from unique structural features that allow for more efficient packing of one component over the other. The structure of MIL-125 and its derivatives contains two types of cages; a large octahedral ($d = 12.5$ Å) and a smaller tetrahedral ($d \sim 6$ Å) cage (see Figure 4.32). Both cages are connected through narrow trigonal windows with an aperture of approximately 6 Å. (Ti)MIL-125-NH_2 displays a preference for *p*-xylene over the other xylene isomers, which decreases in the presence of ethylbenzene and strongly depends on the exact composition of the feed mixture [39]. Other examples relying on differences in the stacking efficiencies of different aromatic C_8 hydrocarbons are known; however, it is difficult to design MOFs showing this type of selectivity because it is highly dependent on the exact geometry and chemical nature of the pores. Among MOFs with the para-selectivity originating from differences in the packing efficiency, MAF-X8 is one of the best performers in the separation of *o*-xylene/*m*-xylene/*p*-xylene/ethylbenzene mixtures [40]. This is attributed to the geometry of the channels in the structure of MAF-X8 that allows for commensurate stacking of *p*-xylene. Calculations suggest that MAF-X8 can outperform state-of-the-art zeolites (e.g. BaX) currently used in

industry for this type of separation, highlighting the potential of MOFs with respect to separation processes.

Another way to realize a high selectivity is to utilize shape-selective effects. Such effects are found for the C_8 aromatics separation using UiO-66 (see Figure 4.28). Molecular simulations and breakthrough experiments show that UiO-66 is highly ortho-selective, while the selectivity in the separation of *p*-xylene/*m*-xylene mixtures is modest [41]. The ortho-selectivity has its origin within the structure of UiO-66. Its **fcu** type structure contains octahedral ($d = 11$ Å) and tetrahedral cages ($d = 8$ Å) connected through narrow windows ($d = 5$–7 Å). The diameter of the tetrahedral cage is within the range of the kinetic diameter of ethylbenzene (6.7 Å), *o*-xylene (7.4 Å), *m*-xylene (7.1 Å), and *p*-xylene (6.7 Å) [42]. The stronger interaction with the bulkier ortho-isomer leads to its preferential adsorption and a selectivity pattern that is inverse to the molecular dimensions [43].

16.2.4 Mixed-Matrix Membranes

With respect to gas separation, membranes offer a number of benefits over packed beds of powders or shaped bodies and other gas separation technologies such as cryogenic distillation or selective condensation, requiring an energy-intensive gas–liquid phase change [44]. Gas separation using membranes does not require a phase change while also allowing for a more compact plant design and operation under continuous steady-state conditions, thus eliminating the need for regeneration of the separation medium. The general principle of membrane separation is shown in Figure 16.9. A feed-stream is passed along one side of the membrane and only one component permeates the membrane while all non-permeating components remain in the feed-stream. The separation process is driven by a pressure difference and the mechanism is strongly dependent on the nature of the material used to manufacture the membrane.

In separation processes using materials with a well-defined pore system such as MOFs and ZIFs adsorption, diffusion, and sometimes molecular sieving dominate the performance of the membrane. In contrast, the separation of gaseous mixtures using polymer membranes is governed by solution-diffusion processes. Early membrane systems include simple materials such as anisotropic cellulose acetate membranes that are applied in the separation of carbon dioxide from natural gas [45]. Today, polymeric membranes are used in many industrial processes, mainly in large-scale gas separation, owing to their facile processing and mechanical strength [46]. Even though polymeric membranes find widespread application they often suffer from low chemical and thermal stability. Additionally, their performance is limited by the Robeson upper boundary, which describes the trade-off between permeability and selectivity [47]. "Inorganic" membranes are made from materials such as zeolites, carbons, and more recently MOFs and ZIFs [48]. They are grouped into two categories: (i) porous inorganic membranes and (ii) dense (nonporous) inorganic membranes. On one hand, these membranes offer unique properties for gas separation such as their high thermal and chemical stability, high gas flux, and high selectivity.

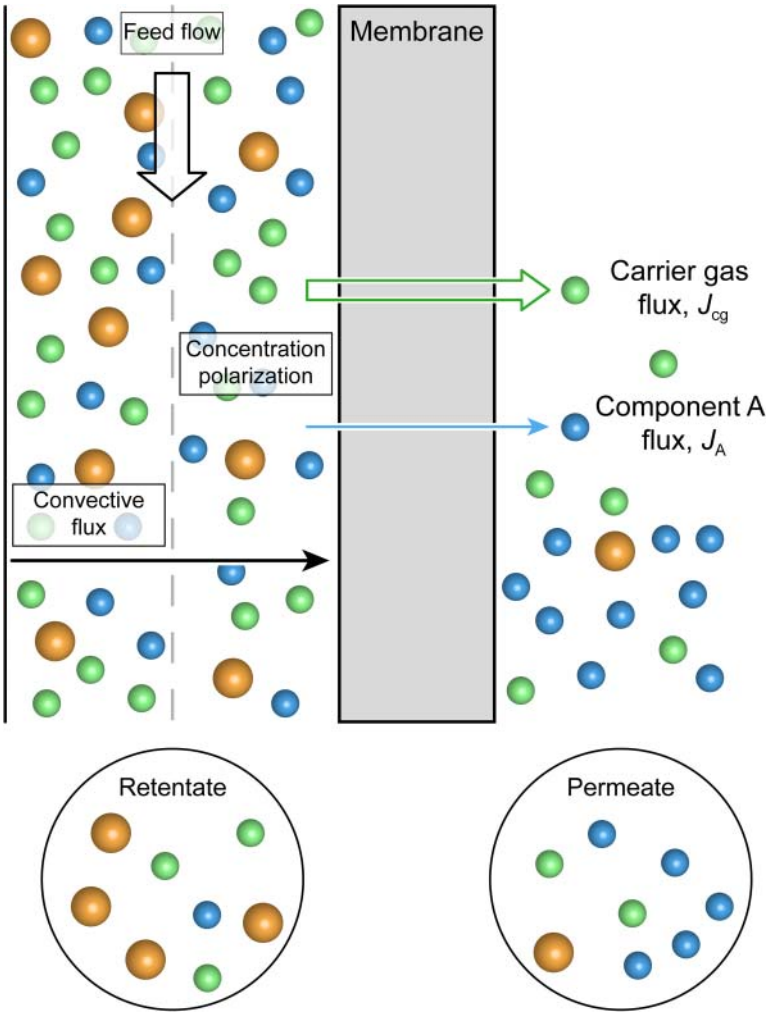

Figure 16.9 Schematic representation of the membrane separation process. A gas mixture that contains three components (gas A, blue; gas B, orange; carrier gas, green) is fed to the separation process. Concentration polarization leads to an increase of component A (c_A) close to the membrane. Gas A permeates the membrane with a larger flux than the carrier gas ($J_A > J_{cg}$) and the membrane is almost impermeable for gas B. The retentate is therefore mainly composed of gas B, whereas the permeate contains mainly gas A.

On the other hand, important factors such as reproducibility, long-term stability, and scalability require further development.

The limitations of polymeric and inorganic membranes are overcome by blending both components in so-called "mixed matrix membranes" (MMMs). These membranes consist of a blend of a polymeric matrix and filler particles (Figure 16.10). This allows them to overcome the Robeson upper boundary for polymeric membranes while avoiding inherent drawbacks common to inorganic membranes such as their brittleness. MMMs combine the facile

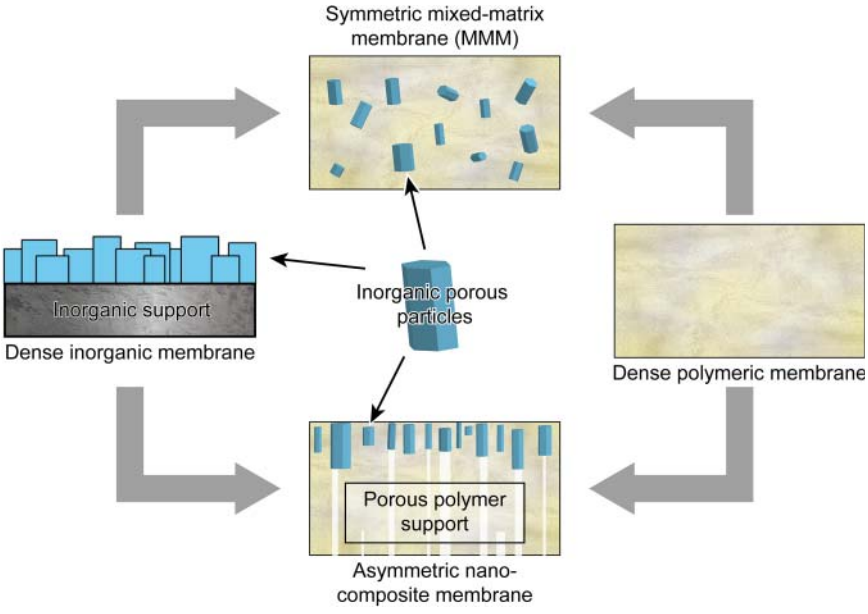

Figure 16.10 Schematic representation of different types of membranes. Both the asymmetric nanocomposite membrane, and the mixed-matrix membrane combine the advantages of polymeric membranes and inorganic porous materials, thereby eliminating the drawbacks presented by both individual methods.

processability and flexibility of polymeric membranes, while augmenting their limited permeability and selectivity with that of the inorganic component (e.g. MOF or ZIF) [45, 46, 47b, 48c, 49]. MOFs and ZIFs are both ideal materials for use as fillers in MMMs. Their synthesis in the form of porous nanoparticles is comparatively facile while the prospect of functionalization allows for the adjustment of structural and electronic features. Current research in this field is focused on enhancing the chemical compatibility between the polymer phase and the porous filler. This is typically realized by modulation of the particle size and size distribution, changes in morphology, judicious functionalization of the organic backbone, and surface modifications. The basic principles of separation are similar to those described "earlier" or "previously"; hence, we will discuss only one representative example. Many review articles addressing MMMs have been published, and the interested reader is referred to these articles [2a, 48c, 49a].

As we saw earlier, many ZIFs are promising candidates in diverse separation processes since they feature certain similarities to zeolites, which have been intensely studied as inorganic fillers for MMMs. ZIFs provide high chemical and thermal stability combined with high selectivity in many separation processes. MMMs of low thickness with enhanced performance and high selectivity compared to their individual components are prepared by embedding submicrometer ZIF-90 ($Zn(aIM)_2$) crystals into poly(imide) membranes [50]. While the adhesion of MOF and ZIF nanoparticles to the polymer blend is commonly challenging, in the case of poly(imide)-ZIF-90 MMMs good adhesion is achieved without any surface modifications.

16.3 Separation in Liquids

The application of MOFs and ZIFs in separation processes is not limited to gaseous mixtures. An increasing interest in the capture of molecules from liquid phase has emerged over the last decade. Two of the most promising applications in this regard are the adsorptive purification of waste water (removal of biologically active molecules and biomolecules) and the adsorptive purification of fuels (removal of cyclic amines), which are both currently performed on a large scale in outdated energy-intensive processes.

As a consequence of the rising world population and the concomitant growing use of medicinal drugs, the concentration of these bioactive molecules and their metabolic products in the water cycle steadily increases. This includes the contamination of surface water, wastewater, groundwater, and to a lesser extent also drinking water [3a]. This not only poses a direct health concern to humans but also has a dramatic impact on the ecosystem [3b–d]. Drinking water is typically purified by filtration, disinfection, and other treatments, such as the removal of organic biologically active molecules using O_3, H_2O_2, UV (ultraviolet) radiation, and their photocatalytic decomposition on TiO_2 or modified TiO_2 surfaces [51]. The more facile nature of adsorptive water purification can substantiate or even substitute these methods and presents the prospect of applying this type of treatment to river or sea water since it does not require a sophisticated infrastructure [52].

Liquid raw fuels typically contain cyclic amines that have adverse effects on the fuels' properties including bad smell, high toxicity, carcinogenicity, and their tendency to form deposits. The combustion of cyclic amines produces nitrous oxides (NO_x) that are one of the main causes of acid rain. Therefore, the removal of nitrogen-containing organic compounds from refinery streams is an important industrial process that is realized by catalytic hydrodenitrogenation (HDN) [53]. This process requires elevated temperatures and pressures, rendering it energy and cost intensive. Additionally, it is accompanied by an undesired decrease in the research octane number (RON) of the fuel. When combining these drawbacks with the fact that the heterocyclic compounds that are removed by HDN have a wide range of applications, it appears profitable to separate them in adsorption-based processes. Such processes not only provide a more energy-efficient alternative to HDM but they also do not result in a decreased RON and allow for the recovery of the cyclic amines.

In the following text we will outline the demands for porous absorbents in both processes regarding their structural features, toxicity, and performance, and give illustrative examples that elaborate the separation mechanisms.

16.3.1 Adsorption of Bioactive Molecules from Water

16.3.1.1 Toxicity of MOFs

For the application of MOFs in the purification of drinking water it is of utmost importance for the material to be hydrolytically stable to ensure that chemicals are not released into the drinking water by dissolution of the MOF. The SBUs in MOFs are often built from heavy metals with relatively high toxicity and many of

the linkers used in MOF synthesis are harmful to humans and aquatic organisms. Therefore, the selection of MOFs constructed from building units that are non-hazardous to health and are stable under application conditions is as important as high selectivity and uptake.

Examples of linker molecules with low toxicity are H_2BDC and H_3BTC [54]. Similarly, metal ions with a high LD_{50} such as Fe, Al, Ti, Mg, and Ca must be selected when targeting MOFs with low toxicity [54b, 55]. Many nontoxic metals tend to form (purely) ionic bonds with carboxylates that render the corresponding MOFs hydrolytically unstable. A more detailed discussion of the hydrolytic stability of MOFs is given in Chapter 17. When nontoxic metal ions and linkers are combined to form framework structures, the resulting MOFs are also expected to display a low overall toxicity. This makes them promising materials for the adsorption-based separation of bioactive molecules in water.

16.3.1.2 Selective Adsorption of Drug Molecules from Water

The adsorption of medical drugs and their metabolic products from water using nontoxic MOFs is not only of interest for the purification of water but, in combination with the appropriate hydrolytic stability/instability, also for the controlled release of drugs in drug delivery systems [54b]. Many studies on adsorption-based separation in aqueous media have been performed using Fe-based MOFs that belong to the MIL series (e.g. MIL-53, MIL-88, MIL-100, and MIL-101) due to their low toxicity and high hydrolytic stability (Figure 16.11).

Figure 16.12 shows a range of drug molecules whose removal from aqueous solution using MOFs has been studied. Naproxene is a nonsteroidal anti-inflammatory drug available as over-the-counter medication, clofibric acid is an herbicide and plant growth regulator, furosemide is a diuretic medication with some veterinary use, sulfalazine is an anti-rheumatoid drug, doxorubine is an anticancer drug, and roxarsone and *p*-arsanilic acid have been used in growing poultry. Studies of the adsorption of these compounds show higher uptakes in MIL-100 and MIL-101 than for other common adsorbents such as activated carbon [56].

The uptake of drug molecules is often correlated to the p*H* of the solution. This is due to interactions arising from pH-dependent structural changes in both the

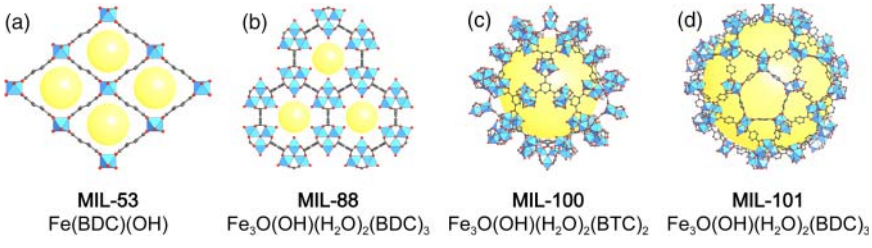

Figure 16.11 Biodegradable porous iron-based frameworks MIL-53, MIL-88, MIL-100 and, MIL-101 (a–d). All MOFs shown are built from iron-based SBUs and nontoxic organic linkers. The large cages of MIL-100 and MIL-101 make them especially interesting for the adsorptive removal of large drug molecules from water.

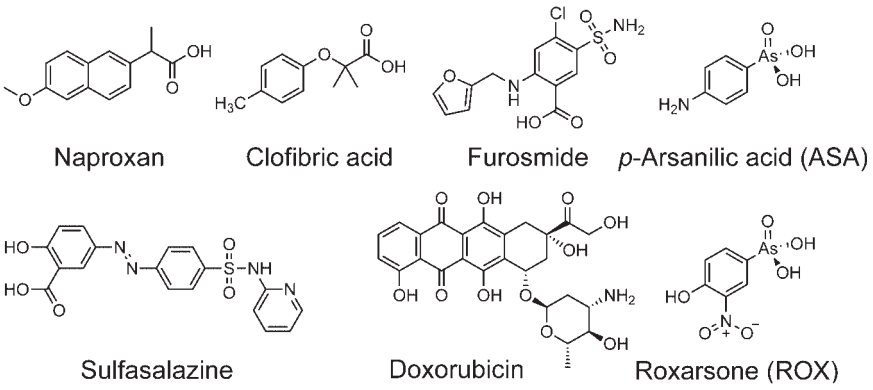

Figure 16.12 Compilation of drug molecules found in drinking water. These molecules are used in farming and human and veterinarian medication.

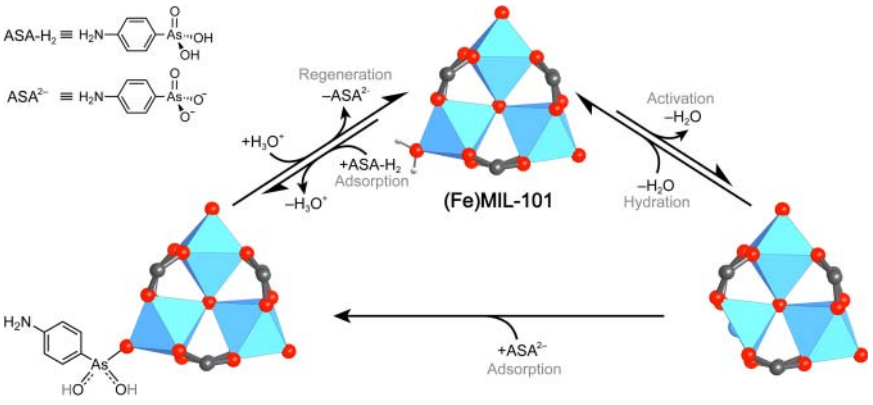

Figure 16.13 Proposed mechanism for the capture of *p*-arsanilic acid (ASA) by (Fe)MIL-101. ASA is adsorbed on the open metal sites of the trinuclear $Fe_3O(H_2O)_2(L)(–COO)_6$ SBU through an equilibrium reaction with water. Controlled release is realized by washing with acidic ethanol and affords the pristine hydrated form of the SBU.

adsorbent and the adsorbate. In most cases, the adsorption of these molecules takes place on the metal centers of the SBU. Figure 16.13 illustrates the mechanism for the adsorption of *p*-arsanilic acid on (Fe)MIL-100 [57].

Choosing a pH range that allows for the existence of a charged form of the adsorbate typically results in a higher uptake. Surface modifications can be used to modify the uptake and adsorption behavior. Such modifications are achieved in a manner akin to that described in Chapters 6, 13, and 14. MIL-101 with ethylenedamine grafted to its open metal sites shows an increased uptake of naproxen due to the stronger interaction of the deprotonated form of naproxen and the protonated amines dangling in the pores at pH of 3–4. In contrast, grafting aminomethanesulfonic acid (taurine) to the open metal sites in the same MOF leads to a significant decrease in the adsorption capacity due to the emergence of repulsive forces.

16.3.1.3 Selective Adsorption of Biomolecules from Water

MOFs can adsorb biomolecules from aqueous solutions, including compounds used in the diagnosis of diseases such as creatinine, a uremic toxin used as a probe for renal failure, and naturally occurring sugars. Of special interest is the separation of xylose. Xylose is a feedstock for the industrial production of furfural, which is further converted to furfuryl alcohol and subsequently used in the production of furan resins [58]. C_5 and C_6 sugars with *cis*-diols (glucose, mannose, and galactose) are known to interact strongly with boronic acid groups ($-BO_2H_2$) [59]. This principle can be implemented into MOF structures by partial replacement of carboxylate-based linkers with analogs bearing boronic acid groups. A MOF designed with this principle in mind is MIL-100(BO_2H_2), where the BTC linker is partially substituted by ditopic H_4BBDC (5-boronobenzene-1,3-dicarboxylate). MIL-100(BO_2H_2) is prepared from metallic chromium, H_4BBDC, and H_3BTC in water and in the presence of HF under hydrothermal conditions. At elevated pH (around 9) it selectively adsorbs galactose from a mixture of xylose, glucose, mannose, and galactose. Its crystallinity and 87% of its initial capacity are retained after regeneration under acidic conditions [60].

16.3.2 Adsorptive Purification of Fuels

HDN is used to remove cyclic amines from liquid fossil fuels [53]. In this process the cyclic amines are converted into ammonia and hydrocarbons. Since *N*-heterocyclic compounds find widespread application in industrial processes, their removal by adsorption and subsequent recovery by desorption appear promising. The adsorptive removal of aromatic *N*-heterocyclic compounds from liquid fossil fuels has been extensively studied since the early 2000s. More recently, the applicability of MOFs and ZIFs in this process has been explored [61]. Here, we will present selected examples illustrating ways to realize the removal of cyclic amines from liquid fuels using MOFs.

16.3.2.1 Aromatic *N*-Heterocyclic Compounds

Aromatic *N*-heterocycles (ANHs) are either basic or nonbasic. In basic ANHs, the lone pair of nitrogen is located in the plane of the molecule and has a basic nucleophilic character. In contrast, the lone pair in nonbasic ANHs is part of the heteroaromatic system and consequently perpendicular to the plane of the molecule. Figure 16.14 shows a selection of basic and nonbasic ANHs that are typically found in liquid fossil fuels.

16.3.2.2 Adsorptive Removal of Aromatic *N*-Heterocycles

Based on the nature of the ANH, different mechanisms predominate for the adsorption. Basic ANHs interact preferentially with Lewis acidic open metal sites. Therefore, the magnitude of the isosteric heat of adsorption in a series of isoreticular frameworks strongly depends on the metal constituting the SBUs. The number of adsorbed molecules is larger than that of the open metal sites. This indicates that there are additional secondary adsorption sites for basic ANHs. In contrast, nonbasic ANHs are adsorbed mainly through hydrogen bonding (polar interactions). This is illustrated by the fact that the uptake

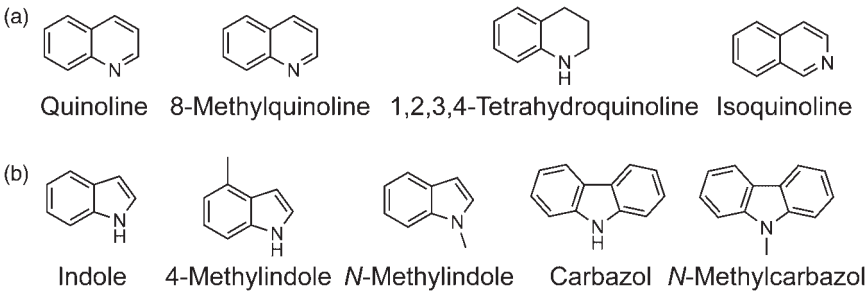

Figure 16.14 Basic (a) and nonbasic (b) aromatic *N*-heterocycles typically found in liquid fossil fuels. While the nitrogen lone pair is located in the plane of the molecule of basic heterocyclic amines, it is part of the aromatic system in nonbasic *N*-heterocycles.

capacity of nonbasic ANHs for a given MOF depends on the polarity of the solvent it is carried out in. The highest uptake is recorded in the presence of the least polar solvents (e.g. *n*-octane). MOFs that are impregnated with acidic molecules such as Keggin type polyoxometallates (e.g. PTA = phosphotungstic acid) display a higher uptake for basic ANH compounds than the pristine MOF. This is due to the stronger acid–base interactions compared to the non-functionalized MOF, whereas a decrease in uptake for nonbasic ANHs results from the smaller accessible pore space.

16.4 Summary

In this chapter, we discussed adsorptive separation processes of gaseous and liquid mixtures. We showed that three different mechanisms can afford the separation of gaseous mixtures (e.g. hydrocarbon mixtures, olefin/paraffin, aromatic C_8 hydrocarbons). The pore size can be adjusted to exclude certain molecules (size exclusion), lead to dissimilar diffusivities for different component of the mixture (kinetic separation), or allow all molecules to diffuse freely in which case the separation is based on adsorption–desorption equilibria (thermodynamic separation). This tailorability of the pore system can in certain structures be carried out anisotropically, which results in anistropic selectivity. The gate opening effect was in many cases shown to increase the selectivity or even enable separation processes that would not be possible in rigid materials. We outlined how the combination of a polymeric membrane and an MOF/ZIF filler can produce MMMs with properties surpassing those of the individual components. We illustrated how MOFs can be used to trap bioactive molecules from water and ANHs from liquid fuels and highlighted the importance of the structural and chemical tunability with respect to these applications.

References

1 (a) Lathia, R.V., Dobariya, K.S., and Patel, A. (2017). *Hydrogen Fuel Cells for Road Vehicles*. Elsevier. (b) Kramer, U., Lorenz, T., Hofmann, C. et al. (2017). Methane number effect on the efficiency of a downsized, dedicated, high performance compressed natural gas (CNG) direct injection engine. SAE Technical Paper 2017-01-0776.

2 (a) Dechnik, J., Gascon, J., Doonan, C. et al. (2017). New directions for mixed-matrix membranes. *Angewandte Chemie International Edition* 56 (32): 9292–9310. (b) Zornoza, B., Tellez, C., Coronas, J. et al. (2013). Metal organic framework based mixed matrix membranes: an increasingly important field of research with a large application potential. *Microporous and Mesoporous Materials* 166: 67–78. (c) Jeazet, H.B.T., Staudt, C., and Janiak, C. (2012). Metal-organic frameworks in mixed-matrix membranes for gas separation. *Dalton Transactions* 41 (46): 14003–14027.

3 (a) World Health Organization (2012). Pharmaceuticals in drinking water. http://www.who.int/water_sanitation_health/publications/pharmaceuticals-in-drinking-water/en/; (accessed 23 March 2018) (b) Cunningham, V.L., Buzby, M., Hutchinson, T. et al. (2006). *Effects of Human Pharmaceuticals on Aquatic Life: Next Steps*. ACS Publications. (c) Fent, K., Weston, A.A., and Caminada, D. (2006). Ecotoxicology of human pharmaceuticals. *Aquatic Toxicology* 76 (2): 122–159. (d) Kidd, K.A., Blanchfield, P.J., Mills, K.H. et al. (2007). Collapse of a fish population after exposure to a synthetic estrogen. *Proceedings of the National Academy of Sciences* 104 (21): 8897–8901.

4 Gaffney, J.S., Streit, G.E., Spall, W.D., and Hall, J.H. (1987). Beyond acid rain. Do soluble oxidants and organic toxinsinteract with SO_2 and NO_x to increase ecosystem effects? *Environmental Science & Technology* 21 (6): 519–524.

5 (a) Szmant, H.H. (1989). *Organic Building Blocks of the Chemical Industry*. Wiley. (b) Weissermel, K. (2008). *Industrial Organic Chemistry*. Wiley.

6 Tomás, R.A.F., Bordado, J.C.M., and Gomes, J.F.P. (2013). *p*-Xylene oxidation to terephthalic acid: a literature review oriented toward process optimization and development. *Chemical Reviews* 113 (10): 7421–7469.

7 Jiang, J. and Sandler, S.I. (2006). Monte Carlo simulation for the adsorption and separation of linear and branched alkanes in IRMOF-1. *Langmuir* 22 (13): 5702–5707.

8 Gutiérrez, I., Díaz, E., Vega, A., and Ordóñez, S. (2013). Consequences of cavity size and chemical environment on the adsorption properties of isoreticular metal-organic frameworks: an inverse gas chromatography study. *Journal of Chromatography A* 1274: 173–180.

9 Farrusseng, D., Daniel, C., Gaudillere, C. et al. (2009). Heats of adsorption for seven gases in three metal-organic frameworks: systematic comparison of experiment and simulation. *Langmuir* 25 (13): 7383–7388.

10 Düren, T. and Snurr, R.Q. (2004). Assessment of isoreticular metal-organic frameworks for adsorption separations: a molecular simulation study of methane/*n*-butane mixtures. *The Journal of Physical Chemistry B* 108 (40): 15703–15708.
11 Düren, T., Sarkisov, L., Yaghi, O.M., and Snurr, R.Q. (2004). Design of new materials for methane storage. *Langmuir* 20 (7): 2683–2689.
12 Ma, S., Wang, X.-S., Collier, C.D. et al. (2007). Ultramicroporous metal-organic framework based on 9,10-anthracenedicarboxylate for selective gas adsorption. *Inorganic Chemistry* 46 (21): 8499–8501.
13 (a) Trung, T.K., Trens, P., Tanchoux, N. et al. (2008). Hydrocarbon adsorption in the flexible metal organic frameworks MIL-53 (Al, Cr). *Journal of the American Chemical Society* 130 (50): 16926–16932. (b) Salles, F., Ghoufi, A., Maurin, G. et al. (2008). Molecular dynamics simulations of breathing MOFs: structural transformations of MIL-53(Cr) upon thermal activation and CO_2 adsorption. *Angewandte Chemie International Edition* 120 (44): 8615–8619.
14 Ma, S., Sun, D., Wang, X.S., and Zhou, H.C. (2007). A mesh-adjustable molecular sieve for general use in gas separation. *Angewandte Chemie International Edition* 46 (14): 2458–2462.
15 (a) Li, J.-R., Kuppler, R.J., and Zhou, H.-C. (2009). Selective gas adsorption and separation in metal-organic frameworks. *Chemical Society Reviews* 38 (5): 1477–1504. (b) Li, B., Wang, H., and Chen, B. (2014). Microporous metal-organic frameworks for gas separation. *Chemistry – An Asian Journal* 9 (6): 1474–1498. (c) Bao, Z., Chang, G., Xing, H. et al. (2016). Potential of microporous metal-organic frameworks for separation of hydrocarbon mixtures. *Energy & Environmental Science* 9 (12): 3612–3641. (d) Wang, Y. and Zhao, D. (2017). Beyond equilibrium: metal-organic frameworks for molecular sieving and kinetic gas separation. *Crystal Growth & Design* 17 (5): 2291–2308. (e) Herm, Z.R., Bloch, E.D., and Long, J.R. (2013). Hydrocarbon separations in metal-organic frameworks. *Chemistry of Materials* 26 (1): 323–338.
16 Eldridge, R.B. (1993). Olefin/paraffin separation technology: a review. *Industrial & Engineering Chemistry Research* 32 (10): 2208–2212.
17 (a) Padin, J., Rege, S.U., Yang, R.T., and Cheng, L.S. (2000). Molecular sieve sorbents for kinetic separation of propane/propylene. *Chemical Engineering Science* 55 (20): 4525–4535. (b) Da Silva, F.A. and Rodrigues, A.E. (1999). Adsorption equilibria and kinetics for propylene and propane over 13X and 4A zeolite pellets. *Industrial & Engineering Chemistry Research* 38 (5): 2051–2057. (c) Rege, S.U., Padin, J., and Yang, R.T. (1998). Olefin/paraffin separations by adsorption: π-complexation vs. kinetic separation. *AIChE Journal* 44 (4): 799–809. (d) Palomino, M., Cantín, A., Corma, A. et al. (2007). Pure silica ITQ-32 zeolite allows separation of linear olefins from paraffins. *Chemical Communications* (12): 1233–1235. (e) Da Silva, F. and Rodrigues, A. (2001). Propylene/propane separation by VSA using commercial 13X zeolite pellets. *AIChE Journal* 47 (2): 341–357. (f) Da Silva, F.A. and Rodrigues, A.E. (2001). Vacuum swing adsorption for propylene/propane separation with 4A zeolite. *Industrial & Engineering Chemistry Research* 40 (24):

5758–5774. (g) Takahashi, A., Yang, R.T., Munson, C.L., and Chinn, D. (2001). Cu(I)-Y-zeolite as a superior adsorbent for diene/olefin separation. *Langmuir* 17 (26): 8405–8413. (h) Bryan, P.F. (2004). Removal of propylene from fuel-grade propane. *Separation and Purification Reviews* 33 (2): 157–182. (i) Narin, G., Martins, V.F., Campo, M. et al. (2014). Light olefins/paraffins separation with 13X zeolite binderless beads. *Separation and Purification Technology* 133: 452–475.

18 (a) Wang, Q.M., Shen, D., Bülow, M. et al. (2002). Metallo-organic molecular sieve for gas separation and purification. *Microporous and Mesoporous Materials* 55 (2): 217–230. (b) Nicholson, T.M. and Bhatia, S.K. (2006). Electrostatically mediated specific adsorption of small molecules in metallo-organic frameworks. *The Journal of Physical Chemistry B* 110 (49): 24834–24836.

19 Nicholson, T.M. and Bhatia, S.K. (2007). Role of electrostatic effects in the pure component and binary adsorption of ethylene and ethane in Cu-tricarboxylate metal-organic frameworks. *Adsorption Science and Technology* 25 (8): 607–619.

20 Lamia, N., Jorge, M., Granato, M.A. et al. (2009). Adsorption of propane, propylene and isobutane on a metal-organic framework: molecular simulation and experiment. *Chemical Engineering Science* 64 (14): 3246–3259.

21 (a) Jorge, M., Lamia, N., and Rodrigues, A.E. (2010). Molecular simulation of propane/propylene separation on the metal-organic framework CuBTC. *Colloids and Surfaces A: Physicochemical and Engineering Aspects* 357 (1): 27–34. (b) Plaza, M., Ferreira, A., Santos, J. et al. (2012). Propane/propylene separation by adsorption using shaped copper trimesate MOF. *Microporous and Mesoporous Materials* 157: 101–111. (c) Rubeš, M., Wiersum, A.D., Llewellyn, P.L. et al. (2013). Adsorption of propane and propylene on CuBTC metal-organic framework: combined theoretical and experimental investigation. *The Journal of Physical Chemistry C* 117 (21): 11159–11167.

22 (a) Hartmann, M., Kunz, S., Himsl, D. et al. (2008). Adsorptive separation of isobutene and isobutane on $Cu_3(BTC)_2$. *Langmuir* 24 (16): 8634–8642. (b) Martins, V.F., Ribeiro, A.M., Ferreira, A. et al. (2015). Ethane/ethylene separation on a copper benzene-1,3,5-tricarboxylate MOF. *Separation and Purification Technology* 149: 445–456.

23 (a) Plaza, M., Ribeiro, A., Ferreira, A. et al. (2012). Separation of C_3/C_4 hydrocarbon mixtures by adsorption using a mesoporous iron MOF: MIL-100 (Fe). *Microporous and Mesoporous Materials* 153: 178–190. (b) Yoon, J.W., Seo, Y.K., Hwang, Y.K. et al. (2010). Controlled reducibility of a metal-organic framework with coordinatively unsaturated sites for preferential gas sorption. *Angewandte Chemie International Edition* 122 (34): 6085–6088. (c) Leclerc, H., Vimont, A., Lavalley, J.-C. et al. (2011). Infrared study of the influence of reducible iron(III) metal sites on the adsorption of CO, CO_2, propane, propene and propyne in the mesoporous metal-organic framework MIL-100. *Physical Chemistry Chemical Physics* 13 (24): 11748–11756. (d) Wuttke, S., Bazin, P., Vimont, A. et al. (2012). Discovering the active sites for C_3 separation in MIL-100(Fe) by using operando IR spectroscopy. *Chemistry – A European Journal* 18 (38): 11959–11967.

24 Liao, P.-Q., Zhang, W.-X., Zhang, J.-P., and Chen, X.-M. (2015). Efficient purification of ethene by an ethane-trapping metal-organic framework. *Nature Communications* 6: 8697.

25 Li, K., Olson, D.H., Seidel, J. et al. (2009). Zeolitic imidazolate frameworks for kinetic separation of propane and propene. *Journal of the American Chemical Society* 131 (30): 10368–10369.

26 Zhang, C., Lively, R.P., Zhang, K. et al. (2012). Unexpected molecular sieving properties of zeolitic imidazolate framework-8. *Journal of Physical Chemistry Letters* 3 (16): 2130–2134.

27 (a) Bux, H., Chmelik, C., Krishna, R., and Caro, J. (2011). Ethene/ethane separation by the MOF membrane ZIF-8: molecular correlation of permeation, adsorption, diffusion. *Journal of Membrane Science* 369 (1): 284–289. (b) Kwon, H.T. and Jeong, H.-K. (2013). Highly propylene-selective supported zeolite-imidazolate framework (ZIF-8) membranes synthesized by rapid microwave-assisted seeding and secondary growth. *Chemical Communications* 49 (37): 3854–3856. (c) Pan, Y., Liu, W., Zhao, Y. et al. (2015). Improved ZIF-8 membrane: effect of activation procedure and determination of diffusivities of light hydrocarbons. *Journal of Membrane Science* 493: 88–96. (d) Verploegh, R.J., Nair, S., and Sholl, D.S. (2015). Temperature and loading-dependent diffusion of light hydrocarbons in ZIF-8 as predicted through fully flexible molecular simulations. *Journal of the American Chemical Society* 137 (50): 15760–15771. (e) Benzaqui, M., Semino, R., Menguy, N. et al. (2016). Toward an understanding of the microstructure and interfacial properties of PIMs/ZIF-8 mixed matrix membranes. *ACS Applied Materials & Interfaces* 8 (40): 27311–27321.

28 Lee, C.Y., Bae, Y.-S., Jeong, N.C. et al. (2011). Kinetic separation of propene and propane in metal-organic frameworks: controlling diffusion rates in plate-shaped crystals via tuning of pore apertures and crystallite aspect ratios. *Journal of the American Chemical Society* 133 (14): 5228–5231.

29 (a) van den Bergh, J., Gücüyener, C., Pidko, E.A. et al. (2011). Understanding the anomalous alkane selectivity of ZIF-7 in the separation of light alkane/alkene mixtures. *Chemistry – A European Journal* 17 (32): 8832–8840. (b) Gücüyener, C., van den Bergh, J., Gascon, J., and Kapteijn, F. (2010). Ethane/ethene separation turned on its head: selective ethane adsorption on the metal-organic framework ZIF-7 through a gate-opening mechanism. *Journal of the American Chemical Society* 132 (50): 17704–17706.

30 Chen, D.-L., Wang, N., Xu, C. et al. (2015). A combined theoretical and experimental analysis on transient breakthroughs of C_2H_6/C_2H_4 in fixed beds packed with ZIF-7. *Microporous and Mesoporous Materials* 208: 55–65.

31 Lan, A., Li, K., Wu, H. et al. (2009). RPM3: a multifunctional microporous MOF with recyclable framework and high H_2 binding energy. *Inorganic Chemistry* 48 (15): 7165–7173.

32 Nijem, N., Wu, H., Canepa, P. et al. (2012). Tuning the gate opening pressure of metal-organic frameworks (MOFs) for the selective separation of hydrocarbons. *Journal of the American Chemical Society* 134 (37): 15201–15204.

33 Cadiau, A., Adil, K., Bhatt, P. et al. (2016). A metal-organic framework-based splitter for separating propylene from propane. *Science* 353 (6295): 137–140.

34 Moreira, M.A., Ferreira, A.F., Santos, J.C. et al. (2014). Hybrid process for *o*- and *p*-xylene production in aromatics plants. *Chemical Engineering and Technology* 37 (9): 1483–1492.

35 Zhang, K., Lively, R.P., Zhang, C. et al. (2013). Exploring the framework hydrophobicity and flexibility of ZIF-8: from biofuel recovery to hydrocarbon separations. *Journal of Physical Chemistry Letters* 4 (21): 3618–3622.

36 Peralta, D., Chaplais, G.r., Simon-Masseron, A.l. et al. (2012). Comparison of the behavior of metal-organic frameworks and zeolites for hydrocarbon separations. *Journal of the American Chemical Society* 134 (19): 8115–8126.

37 Jin, Z., Zhao, H.-Y., Zhao, X.-J. et al. (2010). A novel microporous MOF with the capability of selective adsorption of xylenes. *Chemical Communications* 46 (45): 8612–8614.

38 Vermoortele, F., Maes, M., Moghadam, P.Z. et al. (2011). *p*-Xylene-selective metal-organic frameworks: a case of topology-directed selectivity. *Journal of the American Chemical Society* 133 (46): 18526–18529.

39 Moreira, M.A., Santos, J.C., Ferreira, A.F. et al. (2012). Effect of ethylbenzene in *p*-xylene selectivity of the porous titanium amino terephthalate MIL-125(Ti)_NH_2. *Microporous and Mesoporous Materials* 158: 229–234.

40 Torres-Knoop, A., Krishna, R., and Dubbeldam, D. (2014). Separating xylene isomers by commensurate stacking of *p*-xylene within channels of MAF-X8. *Angewandte Chemie International Edition* 53 (30): 7774–7778.

41 (a) Chang, N. and Yan, X.-P. (2012). Exploring reverse shape selectivity and molecular sieving effect of metal-organic framework UIO-66 coated capillary column for gas chromatographic separation. *Journal of Chromatography A* 1257: 116–124. (b) Granato, M.A., Martins, V.D., Ferreira, A.F.P., and Rodrigues, A.E. (2014). Adsorption of xylene isomers in MOF UiO-66 by molecular simulation. *Microporous and Mesoporous Materials* 190: 165–170.

42 Cavka, J.H., Jakobsen, S., Olsbye, U. et al. (2008). A new zirconium inorganic building brick forming metal organic frameworks with exceptional stability. *Journal of the American Chemical Society* 130 (42): 13850–13851.

43 Bárcia, P.S., Guimarães, D., Mendes, P.A. et al. (2011). Reverse shape selectivity in the adsorption of hexane and xylene isomers in MOF UiO-66. *Microporous and Mesoporous Materials* 139 (1): 67–73.

44 Bernardo, P., Drioli, E., and Golemme, G. (2009). Membrane gas separation: a review/state of the art. *Industrial & Engineering Chemistry Research* 48: 4638–4663.

45 Baker, R.W. (2002). Future directions of membrane gas separation technology. *Industrial and Engineering Chemistry Research* 41 (6): 1393–1411.

46 (a) Aroon, M.A., Ismail, A.F., Matsuura, T., and Montazer-Rahmati, M.M. (2010). Performance studies of mixed matrix membranes for gas separation: a review. *Separation and Purification Technology* 75 (3): 229–242. (b) Ulbricht, M. (2006). Advanced functional polymer membranes. *Polymer* 47 (7): 2217–2262.

47 (a) Robeson, L.M. (1999). Polymer membranes for gas separation. *Current Opinion in Solid State and Materials Science* 4 (6): 549–552. (b) Robeson, L.M. (2008). The upper bound revisited. *Journal of Membrane Science* 320 (1): 390–400.

48 (a) Bastani, D., Esmaeili, N., and Asadollahi, M. (2013). Polymeric mixed matrix membranes containing zeolites as a filler for gas separation applications: a review. *Journal of Industrial and Engineering Chemistry* 19 (2): 375–393. (b) Saufi, S.M. and Ismail, A.F. (2002). Development and characterization of polyacrylonitrile (PAN) based carbon hollow fiber membrane. *Songklanakarin Journal of Science and Technology* 24: 843–854. (c) Seoane, B., Coronas, J., Gascon, I. et al. (2015). Metal-organic framework based mixed matrix membranes: a solution for highly efficient CO_2 capture? *Chemical Society Reviews* 44 (8): 2421–2454. (d) Perez, E.V., Balkus, K.J., Ferraris, J.P., and Musselman, I.H. (2009). Mixed-matrix membranes containing MOF-5 for gas separations. *Journal of Membrane Science* 328 (1): 165–173. (e) Bux, H., Liang, F., Li, Y. et al. (2009). Zeolitic imidazolate framework membrane with molecular sieving properties by microwave-assisted solvothermal synthesis. *Journal of the American Chemical Society* 131 (44): 16000–16001.

49 (a) Zhang, Y., Feng, X., Yuan, S. et al. (2016). Challenges and recent advances in MOF-polymer composite membranes for gas separation. *Inorganic Chemistry Frontiers* 3 (7): 896–909. (b) Chung, T.-S., Jiang, L.Y., Li, Y., and Kulprathipanja, S. (2007). Mixed matrix membranes (MMMs) comprising organic polymers with dispersed inorganic fillers for gas separation. *Progress in Polymer Science* 32 (4): 483–507.

50 Bae, T.H., Lee, J.S., Qiu, W. et al. (2010). A high-performance gas-separation membrane containing submicrometer-sized metal-organic framework crystals. *Angewandte Chemie International Edition* 49 (51): 9863–9866.

51 (a) Balcıoğlu, I.A. and Ötker, M. (2003). Treatment of pharmaceutical wastewater containing antibiotics by O_3 and O_3/H_2O_2 processes. *Chemosphere* 50 (1): 85–95. (b) Saud, P.S., Pant, B., Alam, A.-M. et al. (2015). Carbon quantum dots anchored TiO_2 nanofibers: effective photocatalyst for waste water treatment. *Ceramics International* 41 ((9): 11953–11959. (c) Asghar, A., Raman, A.A.A., and Daud, W.M.A.W. (2015). Advanced oxidation processes for in-situ production of hydrogen peroxide/hydroxyl radical for textile wastewater treatment: a review. *Journal of Cleaner Production* 87: 826–838.

52 Ternes, T.A., Meisenheimer, M., McDowell, D. et al. (2002). Removal of pharmaceuticals during drinking water treatment. *Environmental Science and Technology* 36 (17): 3855–3863.

53 Prins, R. (2001). Catalytic hydrodenitrogenation. *Advances in Catalysis* 46: 399–464.

54 (a) Dai, G., Cui, L., Song, L. et al. (2006). Metabolism of terephthalic acid and its effects on CYP4B1 induction. *Biomedical and Environmental Sciences* 19 (1): 8. (b) Horcajada, P., Chalati, T., Serre, C. et al. (2010). Porous metal-organic-framework nanoscale carriers as a potential platform for drug delivery and imaging. *Nature Materials* 9 (2): 172–178.

55 (a) Singh, R., Gautam, N., Mishra, A., and Gupta, R. (2011). Heavy metals and living systems: an overview. *Indian Journal of Pharmacology* 43 (3): 246. (b) Tchounwou, P.B., Yedjou, C.G., Patlolla, A.K., and Sutton, D.J. (2012). *Molecular, Clinical and Environmental Toxicology*, 133–164. Springer.

56 Cychosz, K.A. and Matzger, A.J. (2010). Water stability of microporous coordination polymers and the adsorption of pharmaceuticals from water. *Langmuir* 26 (22): 17198–17202.

57 Jun, J.W., Tong, M., Jung, B.K. et al. (2015). Effect of central metal ions of analogous metal-organic frameworks on adsorption of organoarsenic compounds from water: plausible mechanism of adsorption and water purification. *Chemistry – A European Journal* 21 (1): 347–354.

58 Kandola, B.K., Ebdon, J.R., and Chowdhury, K.P. (2015). Flame retardance and physical properties of novel cured blends of unsaturated polyester and furan resins. *Polymer* 7 (2): 298–315.

59 Lü, C., Li, H., Wang, H., and Liu, Z. (2013). Probing the interactions between boronic acids and cis-diol-containing biomolecules by affinity capillary electrophoresis. *Analytical Chemistry* 85 (4): 2361–2369.

60 Zhu, X., Gu, J., Zhu, J. et al. (2015). Metal-organic frameworks with boronic acid suspended and their implication for *cis*-diol moieties binding. *Advanced Functional Materials* 25 (25): 3847–3854.

61 (a) Hernández-Maldonado, A.J. and Yang, R.T. (2004). Denitrogenation of transportation fuels by zeolites at ambient temperature and pressure. *Angewandte Chemie International Edition* 116 (8): 1022–1024. (b) Almarri, M., Ma, X., and Song, C. (2009). Role of surface oxygen-containing functional groups in liquid-phase adsorption of nitrogen compounds on carbon-based adsorbents. *Energy & Fuels* 23 (8): 3940–3947.